HHS Public Access

Author manuscript

Soft Matter. Author manuscript; available in PMC 2017 June 19.

Published in final edited form as:

Soft Matter. 2016 August 14; 12(30): 6331–6346. doi:10.1039/c6sm01153e.

111 years of Brownian motion

Xin Bian[a], **Changho Kim**[b], and **George Em Karniadakis**[a]

[a]Division of Applied Mathematics, Brown University, Providence, RI 02912, USA

[b]Lawrence Berkeley National Laboratory, Berkeley, CA 94720, USA

Abstract

We consider the Brownian motion of a particle and present a tutorial review over the last 111 years since Einstein's paper in 1905. We describe Einstein's model, Langevin's model and the hydrodynamic models, with increasing sophistication on the hydrodynamic interactions between the particle and the fluid. In recent years, the effects of interfaces on the nearby Brownian motion have been the focus of several investigations. We summarize various results and discuss some of the controversies associated with new findings about the changes in Brownian motion induced by the interface.

1 Introduction

Soon after the invention of the microscope, the incessant and irregular motion of small grains suspended in a fluid had been observed. It was believed for a while that such jiggling motion was due to living organisms. In 1827, the botanist Robert Brown systematically demonstrated that any small particle suspended in a fluid has such characteristics, even an inorganic grain.[1] Therefore, the explanation for such motion should resort to the realm of physics rather than biology. Since then this phenomenon has been named after the botanist as "Brownian motion".[2] In the classical sense, the phenomenon refers to the random movement of a particle in a medium, *e.g.*, dust in a fluid. However today, its theory can be also applied to describe the fluctuating behavior of a general system interacting with the surroundings, *e.g.*, stock prices.

It was not until 1905 that physicists such as Albert Einstein,[3] William Sutherland,[4] and Marian von Smoluchowski[5] started to gain deep understanding about Brownian motion. While the existence of atoms and molecules was still open to objection, Einstein explained the phenomenon through a microscopic picture. If heat is due to kinetic fluctuations of atoms, the particle of interest, that is, a Brownian particle, should undergo an enormous number of random bombardments by the surrounding fluid particles and its diffusive motion should be observable. The experimental validation of Einstein's theory by Jean Baptiste Perrin unambiguously verified the atomic nature of matter,[6] which was awarded the Nobel Prize in Physics in 1926. Since the seminal works in the 1900s, this subject has fostered many fundamental developments on equilibrium and non-equilibrium statistical physics,[7,8] and enriched the applications of fluid mechanics such as the rheology of suspensions.[9–11] It

Correspondence to: Xin Bian; George Em Karniadakis.

also motivated mathematically rigorous developments of probability theory and stochastic differential equations,[12–14] which in turn boosted the stochastic modeling of finance. For example, one of its remarkable achievements is the Black–Scholes–Merton model for the pricing of options,[15] which was awarded the Nobel Memorial Prize in Economical Sciences in 1997. More recently, Brownian motion has been playing a central and fundamental role in the studies of soft matter and biophysics,[16,17] shifting the subject back to the realm of biology. Other areas of intensive research driven by Brownian motion include the microrheology of viscoelastic materials,[18–21] artificial Brownian motors[22] and self-propelling of active matter,[23,24] fluctuation theorems for states far from equilibrium,[25–27] and quantum fluctuations.[28,29]

In this work, we focus on the classical aspect of Brownian motion based on selective references from 1905 until 2016, which spans the last 111 years. More specifically, we attempt to interpret previous theories from a hydrodynamic perspective. To this end, we mainly consider a spherical particle of sub-micrometer size suspended in a fluid and the particle is subject to free and constrained Brownian motion. Special focus will be given to the velocity autocorrelation function (VACF) of the particle, denoted by $C(t) = \langle \mathbf{v}(0)\cdot\mathbf{v}(t)\rangle$ with the equilibrium ensemble average $\langle\ \rangle$. It measures how similar the velocity $\mathbf{v}$ after time t is to the initial velocity.[30] In general, due to its interaction with the surrounding fluid, the particle's velocity becomes randomized and the magnitude of $\langle \mathbf{v}(0)\cdot\mathbf{v}(t)\rangle$ diminishes as t increases. Compared to the well-known mean-squared displacement (MSD), which is denoted by $\langle \Delta\mathbf{r}^2(t)\rangle$ with the displacement $\Delta\mathbf{r}(t) = \mathbf{r}(t) - \mathbf{r}(0)$, the VACF contains equivalent dynamical information. This can be clearly seen by the following relation:[31,32]

$$\frac{\mathrm{d}}{\mathrm{d}t}\langle \Delta\mathbf{r}^2(t)\rangle = 2\int_0^t C(\tau)\mathrm{d}\tau, \quad (1)$$

which suggests that the VACF can be calculated from the second derivative of the MSD. Nevertheless, the VACF reveals the dynamics in a more direct way; over several time scales of different orders involved, characteristic behaviors of disparate scales may not be clearly differentiated in the MSD, but easily distinguished in the VACF, as will be shown in Fig. 3 of Section 4.

In an order of progressively more accurate hydrodynamic interactions between the particle and the fluid, we organize various theoretical models as follows. At first in Section 2 we introduce the pure diffusion model corresponding to Einstein's microscopic picture. Subsequently, we describe the Langevin model in Section 3, which considers explicitly the inertia of the Brownian particle. We describe the hydrodynamic model in Section 4, which further includes the inertia of the fluid and takes into account the transient hydrodynamic interactions between the particle and the fluid. The persistent VACF from this model has far-reaching consequences for physics. In Section 5, we explore the hydrodynamic model in confinement, with its subtle hydrodynamic interactions among the particle, the fluid and the confining environment. The results of the confined Brownian motion are significant, since the passive microrheology using a Brownian particle to determine interfacial properties has become more and more popular due to its non-intrusive properties. Along the presentation,

we shall focus mainly on the analytical results of the theoretical models and make short excursions to experimental observations and numerical studies. Controversial results will be highlighted. Finally, we conclude this work with some perspectives in Section 6.

2 Pure diffusion

In this section, we summarize Einstein's seminal work in 1905,[†]3 which has two innovative aspects. The first part formulates the diffusion equation to relate the mass diffusion to the MSD, which is a measurable quantity. This relation was also discovered by von Smoluchowski,[5] but with a slightly different factor. The second part is to connect two transport processes: the mass diffusion of the particle and the momentum diffusion of the fluid. Hence, the diffusion coefficient can also be expressed in terms of the fluid properties. The connection between the two transport processes was also obtained by Sutherland independently.[4] In the end of this section, we discuss the validity of the model. By considering the VACF, we demonstrate the limitations of the model and clarify its underlying assumptions.

2.1 Diffusion equation and mean-squared displacement

The probability density function (PDF) $f(x,t)$ of a Brownian particle satisfies the following diffusion equation in the one-dimensional case:

$$\frac{\partial f(x,t)}{\partial t}=D\frac{\partial^2 f(x,t)}{\partial x^2}, \quad (2)$$

where D is the diffusion coefficient of the Brownian particle. This equation is derived under Einstein's microscopic picture by assuming that the difference between $f(x,t+\Delta t)$ and $f(x,t)$ results from the position change Δx of the particle due to random bombardments. D may be expressed in terms of the second moment of Δx and higher moments are dropped off.

For a Brownian particle initially located at the origin, the formal solution to eqn (2) is a Gaussian distribution with mean zero and variance $2Dt$:

$$f(x,t)=\frac{1}{\sqrt{4\pi Dt}}\mathrm{e}^{-\frac{x^2}{4Dt}}. \quad (3)$$

Eqn (3) represents that the PDF of the particle evolves from a Dirac delta function $\delta(x)$ at $t=0$ to a Gaussian distribution with an increasing variance for $t>0$. Accordingly, the MSD of the particle, which is the second moment of the PDF, increases linearly with time:

$$\langle \Delta x^2(t)\rangle = 2Dt. \quad (4)$$

[†]Einstein's works on Brownian motion are collected and translated.[33]

Here, $\Delta x(t) = x(t) - x(0)$ and the brackets denote the ensemble average over the equilibrium distribution. For the three-dimensional case, we have $\langle \Delta x^2 \rangle = \langle \Delta y^2 \rangle = \langle \Delta z^2 \rangle$ and, therefore, for $r = \{x,y,z\}$,

$$\langle \Delta \mathbf{r}^2(t) \rangle = 6Dt. \quad (5)$$

For a random walk like Brownian motion, both the velocity and displacement of the particle are averaged to be zero. Therefore, the simplest but still meaningful measurement is the MSD, which determines the diffusion coefficient *via* eqn (4).

2.2 Stokes–Einstein–Sutherland equation

In a dilute suspension of Brownian particles, the osmotic pressure force acting on individual particles is $-\nabla V$, where V is a thermodynamic potential. Hence, the steady flux of particles driven by this force is $-\phi\mu^{-1}\nabla V$, where ϕ is the particle volume concentration and μ is the mobility coefficient of individual particles. At equilibrium, the flux due to the potential force must be balanced by a diffusional flux as:

$$-\phi\mu^{-1}\nabla V = -D\nabla\phi. \quad (6)$$

Moreover, the concentration should have the form of $\phi \propto \mathrm{e}^{-V/k_\mathrm{B}T}$ at equilibrium, where k_B is Boltzmann's constant and T is the temperature. By substituting the expression of ϕ into eqn (6), we obtain Einstein's relation:

$$D = \mu k_\mathrm{B} T. \quad (7)$$

The mobility coefficient μ is the reciprocal of the friction coefficient ξ. Here, the definitions of μ and ξ arise from a situation where the particle moves at terminal drift velocity v_d in a fluid under a weak external force F_ext: $\mu = \xi^{-1} = v_\mathrm{d}/F_\mathrm{ext}$.

According to Stokes' law,[‡]34 the mobility of a sphere in an incompressible fluid at steady state is

$$\mu = \xi^{-1} = \frac{1}{6\pi\eta a}\frac{1+3\eta/\alpha a}{1+2\eta/\alpha a}, \quad (8)$$

where η is the dynamic viscosity of the fluid, a is the radius of the particle, and α is the friction coefficient at the solid–fluid interface. Note that the Navier slip length is defined as $b = \eta/\alpha$.[35] For $\alpha = 0$, it corresponds to a perfect slip interface, whereas $\alpha = \infty$ corresponds to the no-slip boundary condition originally adopted by George Gabriel Stokes in 1851.[36]

[‡]Stokes' law is valid for the Knudsen number $\mathrm{Kn} = \lambda/a \ll 1$, where λ is the mean free path of fluid particles.[37]

The mobility of a sphere with partial slip may also be determined in eqn (8) by the slip length b.

By combining eqn (7) and (8), we arrive at the celebrated Stokes–Einstein–Sutherland formula[3,4]

$$D=\begin{cases}\frac{k_{\mathrm{B}}T}{4\pi\eta a}, & b=\infty,\\ \frac{k_{\mathrm{B}}T}{6\pi\eta a}, & b=0.\end{cases} \quad (9)$$

This equation establishes the connection between the mass transport of the particle and momentum transport of the fluid. Therefore, one can attain one unknown quantity from the other available quantities *via* eqn (9). For example, given the known values of $k_{\mathrm{B}}T$ and η, and further D from eqn (5), one may determine the radius a of the Brownian particle.[3]

Alternatively, if a is known, Avogadro's number N_{A} can be determined by using the fact $k_{\mathrm{B}} = R_{\mathrm{g}}/N_{\mathrm{A}}$, where R_{g} is the gas constant.[3] Jean Baptiste Perrin actually followed this proposal and determined Avogadro's number ($N = 6.022 \times 10^{23}$ mol^{-1}) A within 6.3% error,[6] which settled the dispute about the theory on the atomic nature of matter.

2.3 Limitations and underlying assumptions

The main criticism of the diffusion model, as Einstein himself realized later,[38,39] is that the inertia of the particle is neglected. This implies that an infinite force is required to change the velocity of the particle to achieve a random walk at each step. Therefore, its velocity cannot be defined and its trajectories are fractal, as illustrated on the right in Fig. 1. Since an apparent velocity is deduced by two consecutive positions, it really depends on the time-resolution of the observations.[40,41] If the observations are separated by a diffusive time scale as in Einstein's model, the particle appears to walk randomly. From the MSD of the diffusion, we may determine an effective mean velocity over a time interval as $\overline{v}=\sqrt{\Delta x^2}/\Delta t=\sqrt{2D}/\sqrt{\Delta t}$. As $\Delta t\to 0$, this effective velocity diverges and cannot represent the real velocity of the particle. This also explains the early controversial measurements on the actual velocity of the particle.[42,43]

This unphysical feature can also be seen by calculating the VACF from eqn (1) and (5): $\langle \mathbf{v}(0)\cdot\mathbf{v}(t)\rangle = 3D\delta(t)$, where $\delta(t)$ is the Dirac delta function. This means that even after an infinitesimal time, the velocity becomes completely uncorrelated with the previous one. A mathematical model corresponding to this case is a Gaussian white noise process for the velocity. Then, $x(t)$ corresponds to a Wiener process, which is continuous but nowhere differentiable in time.[13]

Physically, however, we should be able to find a time scale $t < \tau_{\mathrm{b}}$ for the ballistic regime,[§]39 where the velocity does not change significantly, that is, $\Delta x(t) \approx v(0)t$, as illustrated on the left in Fig. 1. In Einstein's model, τ_{b} can be chosen from the time scale for the duration of

[§]In general, the ballistic time scale τ_{b} is proportional to the Knudsen number.

successive random bombardments. From the equipartition theorem, we have $\langle v^2 \rangle = k_B T/m$, where m is the mass of the particle. Hence, we obtain the MSD expression in the ballistic regime:

$$\langle \Delta x^2(t) \rangle = \frac{k_B T}{m} t^2. \quad (10)$$

In Einstein's model, the time scale τ_b is neglected (*i.e.*, assuming $\tau_b \to 0$) and the MSD is a completely linear function in time. A century ago, Einstein also did not expect that it would be possible to observe the ballistic regime in practice due to the limitation of experimental facilities. Remarkably, such measurements have recently become realistic in rarefied gas,[44] normal gas[45] and liquid,[46,47] with increasing difficulty for fluids with elevated density due to the diminishing of τ_b. However, the experiment on Brownian particles in a liquid is subtle, as it is currently still difficult to resolve time below the sonic scale.[41] Therefore, the equipartition theorem can only be verified for the total mass of the particle and entrained liquid, but not at the single particle level.[46,47] We shall further discuss the effect of the added mass in Section 4.

In summary, Einstein's pure-diffusion model considers only the independent random bombardments on the particle, but nothing else. Although the resulting MSD expression of eqn (4) or (5) is always valid at a large time, the model has the single time scale of the mass-diffusion process $\tau_D = a^2/D$, which is denoted as the diffusive or Smoluchowski time scale.[48] Moreover, the model disallows a definition of velocity, possesses no ballistic regime, and its VACF does not contain any dynamical information. These issues will be resolved in Langevin's model.

3 Langevin equation

A remedy for the unphysical feature of Einstein's model at the ballistic time scale was proposed by Paul Langevin,[49] which takes into account the inertia of the particle.[¶] In Langevin's formulation, which was thought to be "infinitely simpler" according to himself, the equation of motion for the Brownian particle is formally based on Newton's second law of motion as

$$m\frac{\mathrm{d}^2 x}{\mathrm{d}t^2} = -\xi\frac{\mathrm{d}x}{\mathrm{d}t} + \tilde{F}(t), \quad (11)$$

where m is the mass of the particle, ξ is the friction coefficient defined earlier, and $\tilde{F}(t)$ is a random force on the particle. In this mode, the velocity of the particle $v(t) = \dot{x}(t)$ is well-defined and it is subject to two different types of forces exerted by the surrounding fluid: a friction force and a random force. It is further assumed that the random force is an independent Gaussian white noise process. Hence, $\tilde{F}(t)$ satisfies

[¶]Langevin's work is translated.[50]

$$\langle \tilde{F}(t)\rangle = 0, \langle \tilde{F}(t)\tilde{F}(t')\rangle = \Gamma\delta(t-t'), \quad (12)$$

$$\langle \tilde{F}(t)x(t')\rangle = 0, \langle \tilde{F}(t)v(t')\rangle = 0, \quad (13)$$

where $t \geq t'$ and the noise strength Γ is to be determined below.

From a mathematical point of view, eqn (11) is a stochastic differential equation. Compared to Einstein's model, $x(t)$ has better regularity; $x(t)$ is now differentiable. However, $v(t)$ is continuous but not differentiable just as $x(t)$ in Einstein's model. In general, special care needs to be taken to handle a stochastic differential equation, as the ordinary calculus may not hold. However, since eqn (11) is subject to an additive independent noise $\tilde{F}(t)$, we can still legitimately apply the ordinary calculus to calculate the MSD and the VACF from eqn (11).

3.1 Two regimes of mean-squared displacement

We first derive an expression for the MSD and obtain from it two asymptotic limits at both short-time and long-time scales.

Without loss of generality, we take $x(0) = 0$. After multiplying eqn (11) by x and using the fact that $\frac{\mathrm{d}x^2}{\mathrm{d}t} = 2x\frac{\mathrm{d}x}{\mathrm{d}t}$ and $\frac{\mathrm{d}^2x^2}{\mathrm{d}t^2} = 2\left(\frac{\mathrm{d}x}{\mathrm{d}t}\right)^2 + 2x\frac{\mathrm{d}^2x}{\mathrm{d}t^2}$, we have

$$\frac{m\mathrm{d}^2x^2}{2\,\mathrm{d}t^2} - mv^2 = -\frac{\xi \mathrm{d}x^2}{2\,\mathrm{d}t} + x\tilde{F}(t). \quad (14)$$

By taking the average and using eqn (13), we obtain a differential equation for $z = \frac{\mathrm{d}}{\mathrm{d}t}\langle x^2\rangle$:

$$\frac{m\mathrm{d}z}{2\,\mathrm{d}t} + \frac{\xi}{2}z = k_{\mathrm{B}}T, \quad (15)$$

where the equipartition theorem, $m\langle v^2\rangle = k_{\mathrm{B}}T$, was applied. Since $\langle z(0)\rangle = 2\langle x(0)v(0)\rangle = 0$, the solution to eqn (15) is

$$z(t) = \frac{2k_{\mathrm{B}}T}{\xi}(1 - \mathrm{e}^{-\xi t/m}). \quad (16)$$

By integrating eqn (16), we obtain an expression for the MSD over the entire time range as:[51–53]

$$\langle \Delta x^2(t) \rangle = \frac{2k_B T}{\xi} \left(t - \frac{m}{\xi} + \frac{m}{\xi} e^{-\xi t/m} \right). \quad (17)$$

On the one hand, for $t \gg \tau_B = m/\xi$, the exponential term becomes negligible, and we retrieve Einstein's result eqn (4) from eqn (17):

$$\frac{d}{dt} \langle x^2(t) \rangle = \frac{2k_B T}{\xi} = 2D. \quad (18)$$

This may also be directly obtained by dropping off the exponential term in eqn (16).

On the other hand, for $t \ll \tau_B$ or $t \to 0$, by using the power series $e^{-t} = 1 - t + \frac{t^2}{2!} + O(t^3)$ we obtain from eqn (17)

$$\langle \Delta x^2(t) \rangle = \frac{k_B T}{m} t^2, \quad (19)$$

which is identical to the ballistic regime of eqn (10) discussed in Section 2.3. Hence, we clearly see that Langevin's model can explain the ballistic regime as well as Einstein's long-time result of the MSD. The new relevant time scale is the relaxation time of Brownian motion, $\tau_B = m/\xi$.

3.2 Fluctuation-dissipation theorem, velocity autocorrelation function and diffusion coefficient

Now we turn to the velocity of the Brownian particle, which is the new element in Langevin's model. Furthermore, we may characterize the full dynamics of the particle by the VACF.

Let us rewrite the Langevin equation in terms of velocity:

$$m \frac{dv}{dt} = -\xi v + \tilde{F}(t), \quad (20)$$

which is a first-order inhomogeneous differential equation and has the formal solution:[53,54]

$$v(t) = v(0) e^{-\xi t/m} + \frac{1}{m} \int_0^t d\tau \, e^{-\xi(t-\tau)/m} \tilde{F}(\tau). \quad (21)$$

From this solution, we observe that the average of squared velocity $\langle v^2(t) \rangle$ has three contributions: the first one is $\langle v^2(0) \rangle e^{-2\xi t/m}$ and the second one is the cross term

$\frac{2}{m}e^{-\xi t/m}\int_0^t d\tau\, e^{-\xi(t-\tau)/m}\langle v(0)\tilde{F}(\tau)\rangle$, which becomes zero due to eqn (13). The third contribution is of second order in $\tilde{F}(t)$ and, by making use of eqn (13), we have

$$\frac{1}{m^2}\int_0^t d\tau\, e^{-\xi(t-\tau)/m}\int_0^t d\tau'\, e^{-\xi(t-\tau')/m}\Gamma\delta(\tau-\tau')=\frac{\Gamma}{2\xi m}(1-e^{-2\xi t/m}). \quad (22)$$

Therefore, the mean-squared velocity is

$$\langle v^2(t)\rangle=\langle v^2(0)\rangle e^{-2\xi t/m}+\frac{\Gamma}{2\xi m}(1-e^{-2\xi t/m}). \quad (23)$$

At the long-time limit, we expect the equipartition theorem, $\langle v^2(t)\rangle = k_B T/m$, to be valid. Hence, the equality

$$\Gamma=2\xi k_B T \quad (24)$$

must hold. This represents a fundamental relation named as the fluctuation-dissipation theorem (FDT).[55–57] Roughly speaking, the magnitude of the fluctuation Γ must be balanced by the strength of the dissipation ξ so that temperature is well defined in Langevin's model. Therefore, the pair of friction and random forces acts as a thermostat for a Langevin system. It should not come as a surprise that the frictional force and the random force have such a relation, since they both come from the same origin of interactions between the particle and the surrounding fluid molecules.

From the solution of velocity in eqn (21), we can also calculate the VACF of the particle. After multiplying eqn (21) by $v(0)$, and further taking the average, we obtain

$$C(t)\equiv\langle v(0)v(t)\rangle=\langle v^2(0)\rangle e^{-\xi t/m}=\frac{k_B T}{m}e^{-\xi t/m}. \quad (25)$$

Here, the random force term vanished due to eqn (13) and the equipartition theorem was also used. It is simple to see that $C(t)$ decays exponentially and the relevant time scale is the Brownian relaxation time, $\tau_B = m/\xi$.

If we take the time integral of the VACF, we find

$$\int_0^\infty\langle v(0)v(t)\rangle dt=\frac{k_B T}{m}\int_0^\infty e^{-\xi t/m}dt=\frac{k_B T}{\xi}=D, \quad (26)$$

which is just the diffusion coefficient obtained by Einstein. The relation in eqn (26) is not fortuitous, but known as the simplest example of the fundamental Green–Kubo relations.[58–61] These relate the macroscopic transport coefficients to the correlation

functions of the variables fluctuating due to microscopic processes.[62] Such relations were also postulated by the regression hypothesis of Lars Onsager,[63,64] which states that the decay of the correlations between fluctuating variables follows the macroscopic law of relaxation due to small nonequilibrium disturbances.[‖] The 1968 Nobel Prize in Chemistry was awarded to Onsager to glorify his reciprocal relations in the irreversible process, which also formed the basis for further development of nonequilibrium thermodynamics by Ilya Prigogine and others.[54,65–67]

Similarly to the diffusion in the long-time limit, we may define the time-dependent diffusion coefficient as

$$D(t) \equiv \int_0^t \langle v(0)v(t)\rangle \mathrm{d}\tau = \frac{1}{2}\frac{\mathrm{d}}{\mathrm{d}t}\langle \Delta x^2(t)\rangle = \frac{k_\mathrm{B}T}{\xi}(1-\mathrm{e}^{-\xi t/m}). \quad (27)$$

Note that the equivalence of the two definitions in terms of the VACF and the MSD also follows from eqn (1). For Langevin's model, this equality can be explicitly verified by using eqn (17) and (25).

3.3 Limitations and underlying assumptions

The Langevin model not only recovers the long-time result of Einstein's model, but also produces the correct ballistic regime at a short-time limit. An essential ingredient in the model is that the Brownian particle has an inertia, that is, mass m. As a result, the velocity and the VACF become well-defined and continuous in time. By considering a very small relaxation time $m/\xi \to 0$ in eqn (20), the Langevin dynamics degenerates to be the overdamped Brownian dynamics of Einstein's model.

The limitations of the Langevin model can be revealed by considering a corresponding microscopic model, that is, the Rayleigh gas,[68] which contains ideal gas particles and a massive particle. Several attempts were made to derive the Langevin equation from this microscopic model in the early 1960s.[69,70] It was realized that the derivation is possible if the interaction between the Brownian particle and any gas particle takes place only for a short microscopic time.[68,70] This condition can be rigorously verified under the ideal gas assumption and the infinite mass limit of the Brownian particle (*i.e.*, $m \to \infty$), and thus the microscopic justification of the Langevin equation can be provided through the Rayleigh gas model. For Brownian motion in a real gas or a liquid, a mathematically rigorous justification is intractable. One of the reasons is that if the fluid particles interact among themselves, a collective motion (*e.g.*, correlated collisions) of the fluid particles can occur, which implies that the aforementioned condition may not hold.

We will see in Section 4 that the Langevin description is valid only if the Brownian particle is sufficiently denser than the surrounding fluid, where the inertia of the fluid may be neglected. This fact was exploited in a recent experiment,[45] where a silica bead is trapped by

[‖]Coincidentally, the work of Onsager on Brownian motion and linear response laws was conducted when he was teaching at Brown University, although the latter Brown refers to the businessman and philanthropist Nicholas Brown, Jr.

a harmonic potential[53] in air and the experimental VACF corroborates well the results of the Langevin model.[71] For a general case of arbitrary density, the collective motion of the fluid particles and their inertia should be reconsidered carefully.

4 Hydrodynamic model

Although the VACF of a Brownian particle was never explicitly measured in the first half of the twentieth century due to experimental limitation, it was widely believed to decay exponentially. When a new era of computational science began in the 1950s, this belief was put to the test and it marked the failure of the molecular chaos assumption.[72]

4.1 Observation of algebraic decay in VACFs

Using molecular dynamics (MD) simulations, some pioneers started to realize that the VACF of molecules does not follow strictly an exponential decay, but has a slowly decreasing characteristic. This long persistence was found in fluids described by both the Lennard-Jones potential[73,74] and the hard-core potential.[75,76] A milestone took place in 1970 when Alder and Wainwright[77] delivered a definite answer for the long persistence of the VACF as an algebraic decay, that is, $C(t) \sim t^{-d/2}$ for $t \to \infty$. Here d is the dimension of the problem. Meanwhile this scaling was confirmed by independent numerical simulations of Navier–Stokes equations, which indicate that a (transient) vortex flow pattern forms around a tagged particle.[76,77]

These observations from computer simulations led to many intriguing questions as to what is missing in the Langevin model. The most suspicious assumption of the Langevin model (and also of the Einstein model) is probably that the friction coefficient ξ is taken as the solution of the steady Stokes flow, whereas a Brownian particle undergoes erratic movements constantly. Therefore, the steady friction may be valid only if the surrounding fluid becomes quasi-steady immediately after each movement, or less strictly, before the relaxation time $\tau_B = m/\xi$ of the Brownian particle. This deficiency was already pointed out in the early lectures of Hendrik Lorentz:[**]78 $\xi = 6\pi\eta a$ is a good approximation only when the mass density ratio ρ/ρ_B of the fluid and the Brownian particle is so small that the fluid inertia is negligible. We shall discuss later why this is true.

Since the seminal work of Alder and Wainwright, it was very soon widely acknowledged that unsteady hydrodynamics plays a significant role in the dynamics of the Brownian particle. This motivated many theoretical physicists to work on this subject from various perspectives, and so the algebraic decay was understood by several approaches: a purely hydrodynamic approach based on the linearized Navier–Stokes equations,[80,81] a generalized Langevin equation approach based on the fluctuating hydrodynamics,[82–84] the mode-coupling theory,[85–87] and the kinetic theory.[88] Although these methodologies have different perspectives and mathematical sophistication, all of them respect the inertia of the surrounding fluid and corroborated the same scaling of the asymptotic decay on the VACF.[89]

[**]Lorentz's lectures are translated,[79] see page 93 of the translation.

The bold assumption of quasi-steady state in the Langevin model can be examined only if we consider the unsteady solution of the hydrodynamics, which has been available for more than a century from the independent works of Basset and Boussinesq.

4.2 Boussinesq–Basset force

For a spherical particle undergoing unsteady motion influenced by the inertia of the surrounding fluid, its resistant force was known to Boussinesq and Basset:[90–93]

$$\mathbf{F}(t) = -6\pi\eta a\mathbf{v}(t) - \frac{M}{2}\dot{\mathbf{v}}(t) - 6a^2\sqrt{\pi\eta\rho}\int_0^t \frac{\dot{\mathbf{v}}(\tau)}{\sqrt{t-\tau}}\mathrm{d}\tau, \quad (28)$$

where $M = \frac{4}{3}\pi a^3\rho$ is the mass of the fluid displaced by the particle. Note that eqn (28) is obtained by linearizing (dropping the $\mathbf{v}\cdot\nabla\mathbf{v}$ term) the incompressible Navier–Stokes equations together with the no-slip boundary condition on the particle. For a stationary motion $\dot{\mathbf{v}}(t) = 0$, only the first term on the right-hand side remains, which is just the Stokes friction in eqn (11). The second term is due to the added mass of an inviscid incompressible origin, while the third term is the memory effect of the viscous force from the retarding fluid, which is referred to as the Bousinesq–Basset force.

Now let us discuss when the Bousinesq–Basset force becomes as important as the Stokes friction. Since the former is expressed as a convolution integral, we may understand it better in the frequency domain. By taking the Laplace transform of eqn (28), that is, $\mathbf{F}(\omega) = \int_0^\infty \mathrm{e}^{-\omega t}\mathbf{F}(t)\mathrm{d}t$, we obtain $F(\omega) = -\xi(\omega)\mathbf{v}(\omega)$ with[82]

$$\xi(\omega) = 6\pi\eta a + \frac{M}{2}\omega + 6\pi a^2\sqrt{\eta\rho\omega}. \quad (29)$$

From the transformation, we note that any model with only the steady friction should be considered to be a zero-frequency theory.[80] If we compare the first and third terms on the right-hand side of eqn (29), the latter becomes larger than the former for frequency $\omega > \eta/\rho a^2$, or equivalently for time $t < \rho a^2/\eta$. Since the relaxation time in Langevin eqn (11) is $\tau_B = m/\xi = 2\rho_B a^2/9\eta$, the fluid inertia has non-negligible effects on the dynamics of the Brownian particle for $t < (9\rho/2\rho_B)\tau_B$. Hence, if $9\rho/2\rho_B \ll 1$, the fluid inertia is negligible, which also confirms the insightful remark made earlier by Lorentz.

Alternatively, we may realize the significance of the fluid inertia more directly by considering the vorticity $\omega = \nabla \times \mathbf{u}$, which satisfies the diffusion equation $\partial\omega/\partial t = \nu\nabla^2\omega$,[94] where the kinematic viscosity $\nu = \eta/\rho$. The time scale for the vorticity to travel a distance of the radius of the Brownian particle is $\tau_\nu = a^2/\nu$. For the Langevin model to be valid, it must be $\tau_\nu \ll \tau_B$ or $9\rho/2\rho_B \ll 1$ so that the transient behavior of the fluid plays a negligible role in the particle dynamics. This hydrodynamic argument is also in agreement with the analysis of the molecular theory.[70]

In summary, while the Langevin equation provides a fair approximation for $9\rho/2\rho_B \ll 1$, *e.g.*, a dense particle in gas, it does not apply well to the case of $9\rho/2\rho_B \sim 1$, for example, a pollen particle in water, that is the historic observation recorded by Robert Brown.

4.3 Generalized Langevin equation

Now that the importance of the fluid inertia is recognized, we may discuss the equation of motion for the Brownian particle. For a rigid particle suspended in a continuum fluid described by the fluctuating hydrodynamics,[93] the following generalized Langevin equation can be formulated:[83,84]

$$m\frac{\mathrm{d}\mathbf{v}}{\mathrm{d}t} = -\int_0^t \xi(t-\tau)\mathbf{v}(\tau)\mathrm{d}\tau + \tilde{\mathbf{F}}(t). \quad (30)$$

Compared to the original Langevin eqn (20), eqn (30) is non-Markovian as the friction force is history-dependent. The memory kernel $\xi(t)$ is the inverse Laplace transform of eqn (29). In addition, the random force $\tilde{\mathbf{F}}(t)$ is non-white or colored, which can be observed *via* the fluctuation-dissipation relation[57]

$$\langle \tilde{\mathbf{F}}(0)\cdot\tilde{\mathbf{F}}(t)\rangle = 3k_B T\xi(t). \quad (31)$$

At first glance, eqn (30) seems to be simple. We note, however, that the form is quite general and all the complicated information is hidden in the memory kernel $\xi(t)$ or in the statistics of the random force $\tilde{\mathbf{F}}(t)$.

Although theoretically well known, the colored power spectral density of the thermal noise, which is the Fourier transform of eqn (31), has been confirmed by experiments only recently.[95,96] We also note that the same form of equation as eqn (30) can be obtained from microscopic equations of motion for a Hamiltonian fluid through the Mori–Zwanzig formalism.[97–102] In fact, the emergence of a non-Markovian process is a typical scenario when insignificant variables (fast fluid variables in our case) are eliminated in a Markovian process under coarse-graining.[54]

4.4 Heuristic derivations of the algebraic decay

Here, we discuss how the algebraic decay appears in the generalized Langevin eqn (30), and how it can be explained from a hydrodynamic perspective. The first question can be answered by deriving a differential equation that the VACF $C(t) = \langle \mathbf{v}(0)\cdot\mathbf{v}(t)\rangle$ satisfies. After multiplying eqn (30) by $\mathbf{v}(0)$ and taking averages, we obtain the Volterra equation (also known as the memory function equation[103])

$$m\dot{C}(t) = -\int_0^t \xi(t-\tau)C(\tau)\mathrm{d}\tau. \quad (32)$$

It is known that if either $C(t)$ or $\xi(t)$ decays algebraically, then the other also decays algebraically with the same power law and the opposite sign.[104] From the $\sqrt{\omega}$ term of $\xi(\omega)$ in eqn (29), we know that $\xi(t)$ decays like $t^{-3/2}$ with negative values at large time t. Therefore, it is expected that $C(t)$ also decays like $t^{-3/2}$ but with positive values at large time t. This mathematical argument shows that no matter how small ρ/ρ_B is, the asymptotic decay of the VACF is always algebraic rather than exponential. However, for smaller ρ/ρ_B, the exponential decay yields to algebraic decay later in time and the Langevin model becomes a better approximation.

The persistent scaling of the VACF can also be easily understood by a heuristic hydrodynamic argument. Suppose a particle has initial velocity $\mathbf{v}_0$, due to viscous diffusion, after time t, a vortex ring ($d = 2$) or shell ($d = 3$) with radius $r \sim \sqrt{vt}$ develops. The total mass within the influenced zone is $M^* \sim \rho r^d$. If the surrounding fluid is entrained and moves with the particle at time t, by momentum conservation we have $\mathbf{v}(t) = \frac{m\mathbf{v}_0}{M^*} \sim \frac{m\mathbf{v}_0}{\rho}(vt)^{-d/2}$. Then, it is simple to see that $C(t) \sim (vt)^{-d/2}$. The argument above assumes that the particle does not move when the vortex forms. If the particle moves evidently as the vortex develops, we may still extend this hydrodynamic argument by adding in the self-diffusion constant D of the tagged particle into the scaling so that we have $C(t) \sim [(v + D)t]^{-d/2}$. In fact, by introducing the evolution of the probability distribution function of the tagged particle, the following expression was derived rigorously (one-dimensional case):[87]

$$\lim_{t\to\infty} C(t) = \frac{2k_B T}{3\rho}[4\pi(D+v)t]^{-3/2}. \quad (33)$$

This power law scaling is demonstrated by dissipative particle dynamics simulations in Fig. 2.

If the momentum diffusion is much stronger than the mass diffusion or if the Schmidt number Sc = v/D is very large (*e.g.*, a solid particle suspended in a liquid), we can ignore the contribution of D. Under this condition, which is favored by the linearized hydrodynamics, the full expression of $C(t)$ was derived from the fluctuating hydrodynamics of an incompressible fluid for a neutrally buoyant particle:[83,107]

$$C(t) = \frac{2k_B T}{3m}\left[\frac{1}{3\pi}\int_0^\infty \mathrm{d}x \frac{\sqrt{x}\mathrm{e}^{-xvt/a^2}}{1 + x/3 + x^2/9}\right]. \quad (34)$$

Other than the integral form of eqn (34), an alternative closed form of $C(t)$ is also available.[82,108,109]

We compare the VACF from the hydrodynamics theory with that of Langevin's model in Fig. 3(a). We observe that the Langevin model underestimates the decay rate of the VACF at short time ($t \lesssim \tau_v$) while overestimates it at long time ($t \gtrsim \tau_v$).

4.5 Diffusion coefficient and mean-squared displacement

The time-dependent diffusion coefficient $D(t)$ of a Brownian particle can be obtained directly by integrating eqn (34) as shown in eqn (27). Furthermore, the MSD may also be obtained by further integrating $D(t)$ or directly from the VACF as[110,111]

$$\langle \Delta \mathbf{r}^2(t) \rangle = 2 \int_0^t (t-\tau) C(\tau) \mathrm{d}\tau. \quad (35)$$

The non-diffusive signatures of the MSD and the time-dependent diffusion coefficient due to hydrodynamic memory have been validated for Brownian particles in a suspension probed by dynamic light scattering.[††]107,111 More recently, to avoid any (weak) hydrodynamic interactions between particles, optical trapping interferometry has been applied to a single micrometer particle[112] which is trapped in a weakly harmonic potential.[113] Consequently, the hydrodynamic theory for the non-diffusive regime has been explicitly confirmed with excellent accuracy.[112] We compare the time-dependent diffusion coefficients and MSDs from different theoretical models in Fig. 3(b) and (c). We observe that the $D(t)$ from Langevin's model approaches exponentially fast to Einstein's diffusion coefficient, whereas it takes a substantially longer time for the hydrodynamic model to reach a plateau value.

It is worth noting that even when the fluid inertia is important for the dynamics such as the asymptotic decay of $C(t)$ of the Brownian particle, the equation for the diffusion coefficient $D_\infty = \int_0^\infty C(t)\mathrm{d}t = k_\mathrm{B}T/\xi$ always holds. This means that the steady motion or the zero-frequency mobility component provides the largest displacement and dominates the diffusive process.[83,109] Therefore, the Stokes–Einstein–Sutherland formula in eqn (9) is still correct for a diffusive process, which is universally captured by Einstein's model, Langevin's model and the hydrodynamic model.

4.6 Limitations and underlying assumptions

The heuristic approach above assumes that the long-time decay of the VACF for the particle is solely affected by the dynamics of vortex formation driven by the transversal component of the hydrodynamic equations.[89,116] The longitudinal component drives compressibility effects, which vanish in a sonic time scale, and therefore, they do not contribute to the long-time behavior of the dynamics.[87] If the short-time dynamics is of interest, the compressibility should be reconsidered.

When the fluid is considered mathematically to be incompressible, the particle mass m is augmented by an induced mass $M/2$, where M is the mass of the fluid displaced by the particle.[93] Due to this mathematical treatment, for any infinitesimal time δt, $C(\delta t) = k_\mathrm{B}T/(m + M/2)$. However, the equipartition theorem requires that $C(t)$ starts with $C(0) = k_\mathrm{B}T/m$. Therefore, the incompressible assumption generates a discontinuity of $C(t)$ at short time and violates the equipartition theorem of statistical physics.[‡‡]117,118 A similar paradox was recognized when inverse-transforming eqn (29) to get $\xi(t)$, which is singular at $t = 0$ and

[††]An analytical work on the non-diffusive MSD from the physics community of the former Soviet Union seems to predate other relevant works,[114] and it has been recently translated.[115]

[‡‡]Another contemporary work by Giterman and Gertsenshteĭn[119] was recently brought to attention.[115]

leads to a substantial difference between $\mathbf{v}(0)$ and $\mathbf{v}(\delta t)$ in the case of impulsive particle motion.[89,93] The unphysical consequences at short time may be alleviated by realizing that every fluid is (slightly) compressible. Therefore, we may find a reconciliation of the dynamics from short to long time by considering the propagation of sound waves and incorporating a frequency dependent friction at a frequency similar to the inverse of the sound speed c_s.[80,117,118] For a neutrally buoyant particle, the sound wave dissipates 1/3 of the total energy and the contribution on the VACF from the compressibility effects reads[109,117,118]

$$C^{s}(t)=\frac{k_B T}{3m}\mathrm{e}^{-\frac{3c_s t}{2a}}\left[cos\left(\frac{\sqrt{3}c_s t}{2a}\right)-\sqrt{3}sin\left(\frac{\sqrt{3}c_s t}{2a}\right)\right]. \quad (36)$$

We may see in Fig. 3(a) that adding the compressible correction of eqn (36) to the incompressible VACF of eqn (34) indeed respects the equipartition theorem at short time. The effects of the compressibility are not so apparent for the diffusion coefficient or MSD, as indicated in Fig. 3(b) and (c).

Another interesting phenomenon at the short-time scale due to sound propagation is the "backtracking", which may contribute negatively to the overall friction experienced by the particle.[120,121] From the ratio of the added mass and the particle mass $\frac{M}{2m}=\frac{\rho}{2\rho_B}$, it is simple to see that for a lighter fluid the compressibility becomes less important for the particle dynamics.

Similarly any viscoelasticity effects may be incorporated into the generalized friction at a different frequency after introducing a new relaxation time scale.[80] Moreover, one would need to select a suitable viscoelastic model and also determine its relaxation time by other means. The problem is that viscoelasticity includes a vast range of time scales, but most models do not.

The hydrodynamic theory is based on continuum-fluid mechanics, which necessarily cannot resolve the ballistic motion over $\delta t > 0$ accurately. This fact is indicated in the inset of Fig. 3(c), where the Langevin model shows a finite period for the ballistic regime, whereas the hydrodynamic model deviates from it quickly. In the hydrodynamic model (also in Langevin and Einstein models), we consider only the continuous friction such as the Stokes or Bousinesq–Basset drag on the particle, but ignore the Enskog friction on the Brownian particle due to molecular collisions with the solvent.[122,123]

Here we focused on the translational motion of a single spherical particle with the no-slip boundary condition. There are various extensions based on this simple scenario. For example, for a sphere with the slip or partial-slip boundary condition, the magnitude but not the scaling of the asymptotic decay changes.[80] The dynamics for a particle with an arbitrary shape can be formulated as a similar problem.[83,108,124] The VACF of the angular velocity for a rotating particle may also be calculated with an asymptotic behavior as $C^{R}(t) \propto t^{-5/2}$,[§§]83,125,126 and the non-spherical shape alters only its magnitude but not the power

law.[127] For a test particle immersed in a suspension of particles, the asymptotic power law does not change and its magnitude is obtained by replacing the fluid viscosity with the suspension viscosity.[128,129] The unsteady equation of motion for a sphere in a nonuniform flow is also available.[130] For a Brownian particle of molecular size, the value of its radius or slip length on the surface is always conceptually subtle in a continuum description[131] and needs extra care.

5 Effects of confinement

In the past few decades, the effects of an interface on a nearby Brownian particle have been attracting a lot of attention. On the one hand, it is physically interesting to study the dynamics of the Brownian particle in a confined environment, where the momentum relaxation of the fluid is influenced by the interface. On the other hand, it is practically beneficial to deduce the interfacial properties from the observed dynamics of the Brownian particle, which is analogous to the passive microrheology technique for unbounded viscoelastic characterization.[18] Different from the unbounded case, the motion of a Brownian particle near an interface is strongly influenced by its hydrodynamic interactions with the interface, and its studies date back as early as Hendrik Lorentz's reciprocal theorem.[133,134]

From the unbounded motion of a Brownian particle, we learnt that the diffusive process is dominated by the steady or zero-frequency mobility. This is still true in the confined case. Therefore, at first we may ignore the thermal agitations of the fluid and describe the mobility of a spherical particle immersed in Stokes flow bounded by a plane wall in Sections 5.1 and 5.2. Due to the linearity of Stokes flow, the particle's parallel and perpendicular motions to the wall can be decomposed and handled separately. Subsequently, we will discuss the diffusion and VACFs of a Brownian particle near a wall in Section 5.3, followed by other more sophisticated scenarios revealed in Section 5.4.

5.1 Mobility with no-slip interface

When no-slip boundary conditions are assumed on the surfaces of both the particle and the wall, Hiding Faxén derived an expression for the mobility coefficient $\mu_{\parallel}$ of the parallel motion using the method of reflection in his PhD dissertation[135–137]

$$\mu_{\parallel}\left(\frac{a}{h}\right) \approx \mu_{\infty}\left[1-\frac{9}{16}\left(\frac{a}{h}\right)+\frac{1}{8}\left(\frac{a}{h}\right)^{3}-\frac{45}{256}\left(\frac{a}{h}\right)^{4}-\frac{1}{16}\left(\frac{a}{h}\right)^{5}\right], \quad (37)$$

which includes the effects of a second reflection; μ_{∞} is the Stokes mobility coefficient (denoted above as μ) and h is the distance from the center of the sphere to the wall surface. Following the method of reflection applied by Shōichi Wakiya,[138] the mobility coefficient $\mu_{\perp}$ of the perpendicular motion can also be obtained as[139]

§§A slightly earlier work[132] on the rotating motion from the physics community of the former Soviet Union has been recently translated.[115]

$$\mu_{\perp}\left(\frac{a}{h}\right) \approx \mu_{\infty}\left[1-\frac{9}{8}\left(\frac{a}{h}\right)+\frac{1}{2}\left(\frac{a}{h}\right)^{3}\right]. \quad (38)$$

Eqn (37) and (38) represent a hindered motion due to the presence of the wall compared to the mobility coefficient μ_{∞} in the unbounded case. If we truncate eqn (37) and (38) at the first order of a/h, we recover the earlier approximations obtained by the Lorentz's image technique.[134] From these first-order approximations, it is simple to deduce that the perpendicular motion is impeded more strongly than the parallel one. Both the image technique and the method of reflection are only accurate for $a \ll h$.

For the parallel motion, there is no closed form for the solution of mobility over the entire range of h. Instead, Perkin and Jones started out with the Green tensor for a semi-infinite fluid and matched a series result (at large h) with an asymptotic one derived from lubrication theory (at small h) to get the mobility valid for a wide range of h[140,141]

$$\mu_{\parallel}^{-1}\left(\tfrac{a}{h}\right) \approx 1-\tfrac{8}{15}ln\left(1-\tfrac{a}{h}\right)+0.029\left(\tfrac{a}{h}\right) +0.04973\left(\tfrac{a}{h}\right)^{2}-0.1249\left(\tfrac{a}{h}\right)^{3}, \quad (39)$$

which is more accurate than eqn (37) for small h.

For the perpendicular motion, an exact solution can be obtained using the bi-polar coordinates[142,143]

$$\mu_{\perp}^{-1}\left(\tfrac{a}{h}\right)=\tfrac{1}{\mu_{\infty}} \times \tfrac{4}{3}sinh\,\alpha\sum_{n=1}^{\infty}\frac{n(n+1)}{(2n-1)(2n+3)} \times\left[\frac{2\,sinh\,(2n+1)\alpha+(2n+1)\,sinh\,2\alpha}{4\,sinh^{2}\left(n+\frac{1}{2}\right)\alpha-(2n+1)^{2}sinh^{2}\alpha}-1\right], \quad (40)$$

where $\alpha = \cosh^{-1}(h/a)$. Although eqn (40) was immediately validated by experiments,[144] it is expressed as an infinite series, which is inconvenient as a reference solution. An appropriate form as a good approximation to eqn (40) may be obtained by the regression method[145,146]

$$\mu_{\perp}\left(\frac{a}{h}\right) \approx \frac{6-10\,(a/h)+4\,(a/h)^{2}}{6-3\,(a/h)-(a/h)^{2}}. \quad (41)$$

We summarize different approximations for the mobility hampered by a no-slip plane wall in Fig. 4. The results from different methods agree with each other at the intermediate and large distance, that is, $\mu_{\parallel}$ with $h/a \gtrsim 1.5$ and $\mu\perp$ with $h/a \gtrsim 3$. Differences appear only at the short distance; Lorentz's image technique is not accurate for either $\mu_{\parallel}$ or $\mu\perp$. The method of reflection improves the accuracy of $\mu_{\parallel}$, but fails at the lubrication regime ($h/a < 1.1$), which

is covered by eqn (39) of Perkins and Jones. The method of reflection in eqn (38) overcompensates the deviation on $\mu_{\perp}$ from Lorentz's image technique. Adding only a few terms of the series in eqn (40) already provides a convergent value for $\mu_{\perp}$, which is readily represented by the regression form of eqn (41).

5.2 Mobility with slip interface

Although the no-slip boundary condition on the fluid–solid interface cannot be justified from first principles, classical experiments over several decades indeed support its validity, and the no-slip boundary condition has become a cornerstone of continuum-fluid mechanics.[31,37,147,148] However, many recent experiments indicate violations of the no-slip boundary condition in micro-channels even of the micrometer scale.[149–152] Since the slip length of the interface may depend on the shear rate[153] and dynamic response of gas bubbles,[154] any external perturbation from measurements, such as shear flow, could affect the intrinsic properties of the interface. A passive Brownian particle may be an effective probe to sense the interfacial properties locally, as it only leads to a minimal intrusion to the natural environment near the interface.

We again start with a spherical particle immersed in Stokes flow bounded by a single plane wall. The no-slip boundary condition still applies to the particle surface, whereas for the plane wall we define the slip-length b from its boundary condition as[35,148]

$$u_{\perp}=0, \quad \mathbf{u}_{\parallel}=b\frac{\partial \mathbf{u}_{\parallel}}{\partial_n}, \tag{42}$$

where n is the normal direction to the wall. This is the same definition as for the slip length of a particle in eqn (8); the normal component of the velocity vanishes at the interface, whereas the tangential component extrapolates linearly to vanish at distance b inside the solid. For a small slip length $b \ll h$, Lauga and Squires applied the image technique ($a \ll h$) to obtain[155]

$$\mu_{\parallel}\left(\frac{a}{h},\frac{b}{h}\right)\approx\mu_{\infty}\left[1-\frac{9}{16}\left(\frac{a}{h}\right)\left(1-\frac{b}{h}\right)\right], \tag{43}$$

$$\mu_{\perp}\left(\frac{a}{h},\frac{b}{h}\right)\approx\mu_{\infty}\left[1-\frac{9}{8}\left(\frac{a}{h}\right)\left(1-\frac{b}{h}\right)\right], \tag{44}$$

where the mobility coefficients are now functions of both a/h and b/h. For a no-slip wall $b = 0$, eqn (43) and (44) reduce to eqn (37) and (38) to the first order of a/h.

For a large slip length $b \gg h$ (and $a \ll h$), another asymptotic limit is obtained[155]

$$\mu_{\parallel}\left(\frac{a}{h},\frac{b}{h}\right)\approx\mu_{\infty}\left[1+\frac{3}{8}\left(\frac{a}{h}\right)\left(1+\frac{5h}{b}ln\frac{h}{b}\right)\right], \quad (45)$$

$$\mu_{\perp}\left(\frac{a}{h},\frac{b}{h}\right)\approx\mu_{\infty}\left[1-\frac{3}{4}\left(\frac{a}{h}\right)\left(1+\frac{h}{4b}\right)\right]. \quad (46)$$

For $b\rightarrow\infty$, the terms of h/b disappear in eqn (45) and (46) and the mobility for a perfect slip wall is recovered. In this case, eqn (46) corroborates the pioneering work of Brenner.[142]

The higher-order terms are not included in these solutions and the results are accurate only to the first order of a/h and b/h (small slip length) or h/b (large slip length). We summarize the first-order modifications for the mobility of a particle near a wall with a slip boundary condition in Fig. 5. Due to the image technique, the further away from the wall the particle is located (larger h/a), the more accurate are the solutions. In general, the larger the slip length of the wall is, the stronger mobility a nearby particle has. It is worthwhile to note that a large slip length $b/h > 1$ (*e.g.*, $b/h = 50$ or ∞) may cause the parallel mobility coefficient to be even greater than that of the unbounded case as shown in Fig. 5(a), whereas it does not affect the perpendicular mobility significantly as indicated in Fig. 5(b). Therefore, we suggest that the parallel motion of the particle should be probed preferably to determine the interfacial properties, as it is more sensitive to the slip length of the interface and provides a much wider range of mobility coefficients for measurements.

So far, we have assumed that the particle surface has a no-slip boundary condition. Even if the particle–fluid interface also possesses a slip length, the Stokeslet (Green's function) in the image technique does not change.[155] Therefore, the mobility modifications due to the slip wall in eqn (43)–(46) still hold. In this case, we only need to replace μ_{∞} in these equations by the one presented in eqn (8), which takes into account the modifications induced by the slip length at the particle surface.

5.3 Diffusion coefficient and asymptotic decay of VACFs

From the mobility coefficients we may write down the diffusion coefficients for a particle in the vicinity of a plane wall as

$$D_{\parallel}\left(\frac{a}{h}\right)=\mu_{\parallel}\left(\frac{a}{h}\right)k_{\mathrm{B}}T, \quad (47)$$

$$D_{\perp}\left(\frac{a}{h}\right)=\mu_{\perp}\left(\frac{a}{h}\right)k_{\mathrm{B}}T. \quad (48)$$

For the diffusion coefficients of a spherical particle near a plane wall with the no-slip boundary condition, these analytical expressions have been corroborated by experiments,[141,156,157] and fluctuating-hydrodynamics simulations.[158] For a partial-slip wall, the analytical results on parallel mobility are also verified by deterministic continuum simulations.[159]

In Section 4, we have seen that the friction due to the transient dynamics of the fluid plays a significant role in the VACF of the Brownian motion. This is still true in the confined case but more involved. For the unsteady motion of a sphere in viscous flow bounded by a plane wall, where the no-slip boundary condition applies to both solid interfaces, Wakiya calculated the parallel mobility[160,161] and Gotoh and Kaneda worked out the mobility perpendicular to the wall.[162] Further extending the work of Hauge and Martin-Löf[83] based on fluctuating hydrodynamics of the unbounded case, Gotoh and Kaneda obtained the asymptotic VACFs in the confined case with dominant terms as[162]

$$C_{\parallel}(t) \approx \frac{k_{\mathrm{B}}Th^2}{8\rho\pi\sqrt{\pi}}(\nu t)^{-5/2}, \quad (49)$$

$$C_{\perp}(t) \approx \frac{k_{\mathrm{B}}Th^4}{32\rho\pi\sqrt{\pi}}(\nu t)^{-7/2}. \quad (50)$$

These solutions are valid for $t \gg \tau_{\mathrm{h}} = h^2/\nu$, which is the time for the vorticity propagation between the sphere and the wall.

The power laws of $t^{-5/2}$ and $t^{-7/2}$ for the confined VACFs were verified by lattice Boltzmann simulations.[163] However, Felderhof recently claimed that these analytical results are erroneous and the simulations are also too short to achieve an asymptotic limit.[164] Instead, Felderhof performed the calculation himself and found that VACFs behave asymptotically at large t as[164]

$$C_{\parallel}(t) \approx \frac{k_{\mathrm{B}}T(3h^2 - a^2)}{24\rho\pi\sqrt{\pi}}(\nu t)^{-5/2}, \quad (51)$$

$$C_{\perp}(t) \approx -\frac{k_{\mathrm{B}}Ta^2}{24\rho\pi\sqrt{\pi}}(\nu t)^{-5/2} + \frac{k_{\mathrm{B}}Th^4}{32\rho\pi\sqrt{\pi}}(\nu t)^{-7/2} \quad (52)$$

For the parallel motion, the magnitude is slightly different from that of eqn (49). For the perpendicular motion, however, it is even qualitatively different; the long-tail is dominated by a scaling of $t^{-5/2}$ with negative values as in eqn (52) rather than $t^{-7/2}$ with positive values as in eqn (50).

In a recent μs-long molecular dynamics (MD) simulation with Lennard-Jones interactions, the asymptotic scaling of the parallel motion is again confirmed to be $t^{-5/2}$.[165] Furthermore, Huang and Szlufarska utilized a more general result than eqn (51) for a denser particle to validate the magnitude of the asymptotic decay.[165] However, there was still no direct evidence to confirm whether the magnitude in eqn (49) or eqn (51) is more accurate. The Brownian motion was also employed by Huang and Szlufarska to detect a breakdown of the no-slip boundary condition at short time, which demonstrates the capability of a Brownian particle as a probe for the wettability at a liquid–solid interface.

It is still quite challenging to obtain the confined VACFs with a great accuracy from experiments. Available experimental results[157,166] exhibit non-negligible noises, from which neither the scaling nor the magnitude of the VACFs could be conclusive. Therefore, this dispute is yet to be settled.

5.4 Limitations and underlying assumptions

We focused on the mobility of a particle due to a single nearby wall. Effects due to two-wall confinements or two-particle interactions are more involved, but can be tackled.[139,156,159,167–170] We have assumed an incompressible fluid and ignored any compressible behavior of the fluid. For the short-time dynamics, however, sound propagation also plays a decisive role for the Brownian motion in a confined environment,[171–175] just as in the unbounded case.

The random force on a Brownian particle in confinement is also non-white as in the unbounded case. Moreover, the intensity of the power spectral density on position fluctuation or thermal noise is shifted by the wall, as measured experimentally.[96] However, a recent analytical calculation from Felderhof[176] on the spectrum of position fluctuations, where a static wall-slip length is assumed, does not agree with the experimental results. This disagreement suggests that the slip length on the wall is dynamic and introducing a frequency-dependent slip length could potentially improve the modeling based on the continuum fluid mechanics.[153,154,177–181] Nevertheless, it is not certain that this hypothesized continuum boundary condition may faithfully reflect the Brownian motion in a confined fluid at molecular length-time scales, where locking and delayed relaxation caused by the epitaxial ordering of the fluid structure near the interface may be significant.[165,182] Furthermore, the mobility of a Brownian particle due to the atomistic collisions confined in a microscale channel[183] may not always be described by the linearized hydrodynamic equations.

6 Summary and perspectives

We summarized three theoretical models for a Brownian particle suspended in a fluid: Einstein’s model, Langevin’s model, and the hydrodynamic model and its extensions near a confined interface. From the perspective of hydrodynamic interactions between the particle and the fluid, each model is more elaborate than its preceding one.

It is simple to differentiate the capability of different models by taking into account the disparate time scales involved. Einstein’s model considers only the diffusive time scale $\tau_D =$

a^2/D, when the particle undergoes a random walk, and thus a statistical description of its displacements is feasible without involving the momentum coordinates of either the particle or the fluid. Langevin's model introduces the inertia of the particle, and therefore an extra time scale is introduced, $\tau_B = m/\xi$, where ξ is the friction coefficient due to the viscous fluid at steady state. Hence, the model separates two asymptotic regimes, that is, the ballistic regime $t \ll \tau_B$ and the diffusive regime $t \gg \tau_B$. Moreover, due to the particle inertia its velocity is well-defined and the velocity autocorrelation function (VACF) encodes the full dynamics of the particle with an exponential decay. If the relaxation time of the viscous fluid $\tau_V = a^2/\nu$ is comparable to or larger than τ_B, that is $9\rho/2\rho_B \gtrsim 1$, which is a typical scenario for a colloidal suspension (*e.g.*, a pollen particle in water), the inertia of the fluid must be explicitly taken into account. The hydrodynamic model is based on the solution of the linearized Navier–Stokes or unsteady Stokes equations, which is employed to calculate the full dynamics (signified by the VACF) of a Brownian particle. The coupling between the inertias of the particle and the fluid is mediated by their transient hydrodynamic interactions, and this leads to an algebraic decay of the particle's VACF. The power law scaling indicates significant implications, such as the failure of the molecular chaos assumption, which is expected from Langevin's model.

When a Brownian particle jiggles near an interface, the relaxation of the fluid due to vortex development is affected by its encounter with the interface. Naturally, this introduces a new time scale $\tau_h = h^2/\nu$, which indicates the time of vorticity propagation between the particle and the wall. For $t \gg \tau_h$, the asymptotic limit of the VACFs (including parallel and perpendicular components) for the particle may be calculated and they still follow the power law scalings. However, the actual magnitude and power law from analytical approaches remain controversial. Existing results from experiments are also imperfect for a consensus. Perhaps new experimental techniques illustrated by Raizen's and Florin's groups[46,47] may provide a definite answer for the asymptotic limit in the near future. Furthermore, if the sonic time scales in a liquid such as $\tau_{c_s} = a/c_s$ and $\tau'_{c_s} = h/c_s$ are to be considered for the dynamics of a Brownian particle, perhaps extra innovations in experimental facilities are yet to be developed.

Besides the analytical and experimental works, we also wish to emphasize the effectiveness of various numerical methods on the study of Brownian motion. Some popular methods to study the dynamics of a (non-)Brownian suspension include Brownian dynamics,[184] Stokesian dynamics,[185,186] and the force-coupling method,[187–189] which are very efficient for the bulk rheology at quasi-steady state. However, these methods are semi-analytical and rely on the solutions of steady Stokes flow. Therefore, they may not be appropriate for studying the dynamics of Brownian motion involving time scales τ_V or τ_{c_s}. An alternative numerical method being able to consider τ_V explicitly is the boundary integral method,[94] which solves the unsteady Stokes equations. Nevertheless, it is generally difficult to include the compressibility (related dynamics at the sonic time scale τ_{c_s}) and Brownian motion into a boundary integral implementation. With the increasing capacity of parallel computing, it might be tempting to simulate the Brownian motion of a particle by molecular dynamics (MD),[190,191] which may cover the ballistic regime, the sonic time scale as well as the momentum relaxation time of the fluid. A typical colloid of radius 1 μm in water at room

temperature diffuses over its own radius distance in about 5 s. To resolve the stiff vibrations of water molecules in a MD simulation, a numerical time step must be about 10^{-15} s for stability. Therefore, it is still impractical to simulate such a simple scenario with a full atomistic description. The most realistic class of numerical methods to study the Brownian motion and its relevant areas seems to be the mesoscopic methods, which may cover a wide range of spatial-temporal scales. This category includes the mesh-based methods, such as finite difference,[192] finite volume,[193–195] and lattice Boltzmann,[196,197] and also the particle-based methods, such as dissipative particle dynamics,[198] smoothed particle hydrodynamics,[158,199] and stochastic rotation dynamics/multiple-particle collision dynamics.[200–202]

Acknowledgments

We would like to thank Prof. Bruce Caswell for a critical reading of the manuscript. This work was primarily supported by the Computational Mathematics Program within the Department of Energy office of Advanced Scientific Computing Research as part of the Collaboratory on Mathematics for Mesoscopic Modeling of Materials (CM4). This work was also sponsored by the U.S. Army Research Laboratory and was accomplished under Cooperative Agreement Number W911NF-12-2-0023. This research was also partially supported by the grants U01HL114476 and U01HL116323 from the National Institutes of Health.

Biographies

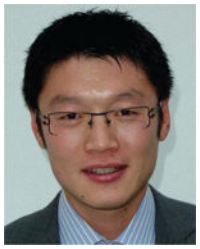

Xin Bian received his PhD in 2015 from Technische Universität München and is a postdoctoral research associate in the Division of Applied Mathematics at Brown University. His research focuses on multiscale modeling and simulation of soft matter physics.

Changho Kim received his PhD in 2015 from Brown University and is a postdoctoral researcher in the Computational Research Division at the Lawrence Berkeley National Laboratory. His research areas include molecular theory and simulation, and mesoscopic modeling of soft materials.

George Em Karniadakis received his PhD in 1987 from Massachusetts Institute of Technology and is the Charles Pitts Robinson and John Palmer Barstow Professor of Applied Mathematics at Brown University. His research interests include diverse topics in computational science both on algorithms and applications. A main current thrust is stochastic simulations and multiscale modeling of physical and biological systems.

References

1. Brown, R. The miscellaneous botanical works of Robert Brown. Vol. I. The Ray Society; London: 1866.
2. Haw MD. J Phys.: Condens Matter. 2002; 14:7769.
3. Einstein A. Ann Phys. 1905; 322:549–560.
4. Sutherland W. Philos Mag. 1905; 9:781–785.
5. von Smoluchowski M. Ann Phys. 1906; 326:756–780.
6. Perrin J. Ann Chim Phys. 1909; 18:1–144.
7. Kubo R. Science. 1986; 233:330–334. [PubMed: 17737620]
8. Hänggi P, Marchesoni F. Chaos. 2005; 15:026101.
9. Einstein A. Ann Phys. 1906; 324:289–306.
10. Batchelor GK. J Fluid Mech. 1977; 83:97–117.
11. Mewis, J., Wagner, NJ. Colloidal suspension rheology. Cambridge University Press; Cambridge: 2012.
12. Stratonovich, RL. Introduction to the theory of random noise. Gordon and Breach; New York, London: 1963.
13. Nelson, E. Dynamic theories of Brownian motion. Princeton University Press; 1967.
14. Gardiner, CW. Handbook of stochastic methods for physics, chemistry and the natural sciences. 3rd. Springer-Verlag; Berlin Heidelberg: 2004.
15. Black F, Scholes M. J Polit Econ. 1973; 81:637–654.
16. Frey E, Kroy K. Ann Phys. 2005; 14:20–50.
17. Li X, Vlahovska PM, Karniadakis GE. Soft Matter. 2013; 9:28–37. [PubMed: 23230450]
18. Mason TG, Weitz DA. Phys Rev Lett. 1995; 74:1250–1253. [PubMed: 10058972]
19. Waigh TA. Rep Prog Phys. 2005; 68:685.
20. Cicuta P, Donald AM. Soft Matter. 2007; 3:1449–1455.
21. Squires TM, Mason TG. Annu Rev Fluid Mech. 2010; 42:413–438.
22. Hänggi P, Marchesoni F. Rev Mod Phys. 2009; 81:387–442.
23. Marchetti MC, Joanny JF, Ramaswamy S, Liverpool TB, Prost J, Rao M, Simha RA. Rev Mod Phys. 2013; 85:1143–1189.
24. Elgeti J, Winkler RG, Gompper G. Rep Prog Phys. 2015; 78:056601. [PubMed: 25919479]
25. Evans, DJ., Morriss, G. Statistical mechanics of nonequilibrium liquids. 2nd. Cambridge University Press; 2008.
26. Seifert U. Rep Prog Phys. 2012; 75:126001. [PubMed: 23168354]
27. Bertini L, De Sole A, Gabrielli D, Jona-Lasinio G, Landim C. Rev Mod Phys. 2015; 87:593–636.

28. Gardiner, CW., Zoller, P. Quantum noise: a handbook of Markovian and non-Markovian quantum stochastic methods with applications to quantum optics. Springer-Verlag; Berlin Heidelberg: 2000.
29. Campisi M, Hänggi P, Talkner P. Rev Mod Phys. 2011; 83:771–791.
30. Taylor GI. Proc London Math Soc. 1922; s2–20:196–212.
31. Hansen, JP., McDonald, IR. Theory of simple liquids. 4th. Elsevier; 2013.
32. Kim C, Borodin O, Karniadakis GE. J Comput Phys. 2015; 302:485–508.
33. Fürth, R., Cowper, AD. Investigations on the theory of the Brownian movement. Dover Publications, Inc; 1956.
34. Batchelor, GK. An introduction to fluid dynamics. Cambridge University Press; Cambridge: 2000. First Cambridge Mathematical Library edn
35. Navier CL. Mém Acad R Sci Ints Fr. 1823; 6:389–440.
36. Stokes GG. Trans Cambridge Philos Soc. 1851; 9:8.
37. Karniadakis, GE., Beskok, A., Aluru, N. Microflows and nanoflows: fundamentals and simulation. Springer; New York: 2005.
38. Einstein A. Ann Phys. 1906; 324:371–381.
39. Einstein A. Z Elektrochem Angew Phys Chem. 1907; 13:41–42.
40. Pusey PN. Science. 2011; 332:802–803. [PubMed: 21566182]
41. Li T, Raizen MG. Ann Phys. 2013; 525:281–295.
42. Exner FM. Ann Phys. 1900; 307:843–847.
43. Kerker M. J Chem Educ. 1974; 51:764.
44. Blum J, Bruns S, Rademacher D, Voss A, Willenberg B, Krause M. Phys Rev Lett. 2006; 97:230601. [PubMed: 17280186]
45. Li T, Kheifets S, Medellin D, Raizen MG. Science. 2010; 328:1673–1675. [PubMed: 20488989]
46. Huang R, Chavez I, Taute KM, Lukic B, Jeney S, Raizen MG, Florin EL. Nat Phys. 2011; 7:576–580.
47. Kheifets S, Simha A, Melin K, Li T, Raizen MG. Science. 2014; 343:1493–1496. [PubMed: 24675957]
48. Dhont, JKG. An introduction to dynamics of colloids. Elsevier; Amsterdam: 1996.
49. Langevin P. C R Acad Sci. 1908; 146:530–533.
50. Lemons DS, Gythiel A. Am J Phys. 1997; 65:1079–1081.
51. Ornstein LS. Proc – Acad Sci Amsterdam. 1919; 21:96.
52. Fürth R. Z Phys. 1920; 2:244–256.
53. Uhlenbeck GE, Ornstein LS. Phys Rev. 1930; 36:823–841.
54. Zwanzig, R. Nonequilibrium statistical mechanics. Oxford University Press; 2001.
55. Nyquist H. Phys Rev. 1928; 32:110–113.
56. Callen HB, Welton TA. Phys Rev. 1951; 83:34–40.
57. Kubo R. Rep Prog Phys. 1966; 29:255.
58. Green MS. J Chem Phys. 1952; 20:1281–1295.
59. Green MS. J Chem Phys. 1954; 22:398–413.
60. Kubo R, Tomita K. J Phys Soc Jpn. 1954; 9:888–919.
61. Kubo R. J Phys Soc Jpn. 1957; 12:570–586.
62. Zwanzig R. Annu Rev Phys Chem. 1965; 16:67–102.
63. Onsager L. Phys Rev. 1931; 37:405–426.
64. Onsager L. Phys Rev. 1931; 38:2265–2279.
65. De Groot, SR., Mazur, P. Non-equilibrium thermodynamics. Dover Publications, Inc; New York: 1962.
66. Prigogine, I. Introduction to thermodynamics of irreversible processes. 3rd. Interscience Publishers, a division of John Wiley & Sons; 1967.
67. Kubo, R., Toda, M., Hashitsume, N. Statistical physics II nonequilibrium statistical mechanics. Springer; 1991.

68. Kim C, Karniadakis GE. Phys Rev E: Stat, Nonlinear, Soft Matter Phys. 2013; 87:032129.
69. Lebowitz JL, Rubin E. Phys Rev. 1963; 131:2381–2396.
70. Mazur P, Oppenheim I. Physica. 1970; 50:241–258.
71. Wang MC, Uhlenbeck GE. Rev Mod Phys. 1945; 17:323–342.
72. Dorfman, JR. An introduction to chaos in nonequilibrium statistical mechanics. Cambridge University Press; 1999.
73. Rahman A. Phys Rev. 1964; 136:A405–A411.
74. Rahman A. J Chem Phys. 1966; 45:2585–2592.
75. Alder BJ, Wainwright TE. Phys Rev Lett. 1967; 18:988–990.
76. Alder BJ, Wainwright TE. Phys Soc Jpn J Sup Proc Inter Conf Statis Mech held 9–14 September, 1968 in Kyoto. 1969; 26:267.
77. Alder BJ, Wainwright TE. Phys Rev A: At, Mol, Opt Phys. 1970; 1:18–21.
78. Lorentz, HA. Lessen over theoretische Natuurkunde V Kinetische Problemen (1911–1912). Voorheen E J Brill; Leiden: 1921.
79. Lorentz, HA. Lectures on theoretical physics (Delivered at the University of Leiden). Macmillan and Co., Limited, St Martin's Street; London: 1927. vol. I Aether Theories and Aether Models, Kinetical Problems
80. Zwanzig R, Bixon M. Phys Rev A: At, Mol, Opt Phys. 1970; 2:2005–2012.
81. Widom A. Phys Rev A: At, Mol, Opt Phys. 1971; 3:1394–1396.
82. Chow TS, Hermans JJ. J Chem Phys. 1972; 57:1799–1800.
83. Hauge EH, Martin-Löf A. J Stat Phys. 1973; 7:259–281.
84. Bedeaux D, Mazur P. Physica. 1974; 76:247–258.
85. Ernst MH, Hauge EH, Van Leeuwen JMJ. Phys Rev Lett. 1970; 25:1254–1256.
86. Ernst MH, Hauge EH, Van Leeuwen JAJ. Phys Lett A. 1971; 34:419–420.
87. Ernst MH, Hauge EH, Van Leeuwen JMJ. Phys Rev A: At, Mol, Opt Phys. 1971; 4:2055–2065.
88. Dorfman JR, Cohen EGD. Phys Rev Lett. 1970; 25:1257–1260.
89. Pomeau Y, Résibois P. Phys Rep. 1975; 19:63–139.
90. Boussinesq JV. C R Acad Bulg Sci. 1885; 100:935–937.
91. Basset, AB. Treatise on hydrodynamics 2. Cambridge: Deighton, Bell and Co.; 1888.
92. Boussinesq, PJ. Théorie analytique de la chaleur, III. Gauthier-Villars; Paris: 1903.
93. Landau, LD., Lifshitz, EM. Fluid mechanics. Vol. 6. Pergamon Press; Oxford: 1959.
94. Pozrikidis, C. Boundary integral and singularity methods for linearized viscous flow (Cambridge Texts in Applied Mathematics). Cambridge University Press; 1992.
95. Franosch T, Grimm M, Belushkin M, Mor FM, Foffi G, Forro L, Jeney S. Nature. 2011; 478:85–88. [PubMed: 21979048]
96. Jannasch A, Mahamdeh M, Schäffer E. Phys Rev Lett. 2011; 107:228301. [PubMed: 22182046]
97. Zwanzig R. Phys Rev. 1961; 124:983–992.
98. Mori H. Prog Theor Phys. 1965; 33:423–455.
99. Chorin AJ, Hald OH, Kupferman R. Proc Natl Acad Sci U S A. 2000; 97:2968–2973. [PubMed: 10737778]
100. Hijón C, Español P, Vanden-Eijnden E, Delgado-Buscalioni R. Faraday Discuss. 2010; 144:301–322. [PubMed: 20158036]
101. Li Z, Bian X, Caswell B, Karniadakis GE. Soft Matter. 2014; 10:8659–8672. [PubMed: 25252001]
102. Li Z, Bian X, Li X, Karniadakis GE. J Chem Phys. 2015; 143:243128. [PubMed: 26723613]
103. Boon, JP., Yip, S. Molecular hydrodynamics. Dover Publications, Inc.; New York: 1991.
104. Corngold N. Phys Rev A: At, Mol, Opt Phys. 1972; 6:1570–1573.
105. Lei H, Fedosov DA, Karniadakis GE. J Comput Phys. 2011; 230:3765–3779. [PubMed: 21499548]
106. Bian X, Deng M, Tang YH, Karniadakis GE. Phys Rev E. 2016; 93:033312. [PubMed: 27078489]

107. Paul GL, Pusey PN. J Phys A: Math Gen. 1981; 14:3301.
108. Hinch EJ. J Fluid Mech. 1975; 72:499–511.
109. Russel WB. Annu Rev Fluid Mech. 1981; 13:425–455.
110. Berne, BJ., Pecora, R. Dynamic light scattering with applications to chemistry, biology, and physics. Dover Publications, Inc; 2000.
111. Weitz DA, Pine DJ, Pusey PN, Tough RJA. Phys Rev Lett. 1989; 63:1747–1750. [PubMed: 10040660]
112. Lukić B, Jeney S, Tischer C, Kulik AJ, Forró L, Florin EL. Phys Rev Lett. 2005; 95:160601. [PubMed: 16241779]
113. Clercx HJH, Schram PPJM. Phys Rev A: At, Mol, Opt Phys. 1992; 46:1942–1950.
114. Vladimirsky V, Terletzky YA. Zh Eksp Theor Fiz. 1945; 15:258–263.
115. Lisy V, Tothova J. arXiv cond-mat/0410222v1. 2004
116. Kadanoff LP, Martin PC. Ann Phys. 1963; 24:419–469.
117. Chow T, Hermans J. Physica. 1973; 65:156–162.
118. Zwanzig R, Bixon M. J Fluid Mech. 1975; 69:21–25.
119. Giterman MS, Gertsenshtein ME. Sov Phys JETP. 1966; 23:722–728.
120. Felderhof BU. J Chem Phys. 2005; 123:044902. [PubMed: 16095387]
121. Lesnicki D, Vuilleumier R, Carof A, Rotenberg B. Phys Rev Lett. 2016; 116:147804. [PubMed: 27104730]
122. Hynes JT. Annu Rev Phys Chem. 1977; 28:301–321.
123. Chapman, S., Cowling, TG., Burnett, D. The mathematical theory of non-uniform gases. Cambridge University Press; 1999.
124. Brenner H. J Colloid Interface Sci. 1967; 23:407–436.
125. Ailawadi NK, Berne BJ. J Chem Phys. 1971; 54:3569–3571.
126. Berne BJ. J Chem Phys. 1972; 56:2164–2168.
127. Cichocki B, Felderhof BU. Physica A. 1995; 213:465–473.
128. Cichocki B, Felderhof BU. Phys Rev E: Stat Phys, Plasmas, Fluids, Relat Interdiscip Top. 1995; 51:5549–5555.
129. Cichocki B, Felderhof BU. Phys Rev E: Stat Phys, Plasmas, Fluids, Relat Interdiscip Top. 2000; 62:5383–5388.
130. Maxey MR, Riley JJ. Phys Fluids. 1983; 26:883–889.
131. Schmidt JR, Skinner JL. J Chem Phys. 2003; 119:8062–8068.
132. Zatovsky AV. Izvestia Vysshikh uchebnykh zavedenii Fizika. 1969:13–17.
133. Lorentz HA. Ein allgemeiner Satz, die Bewegung einer reibenden Flüssigkeit betreffend, nebst einigen Anwendungen desselben. 1896; 5:168–174.
134. Lorentz, HA. Abhandlungen über Theoretische Physik. Verlag Von, BG., editor. Teubner, Leipzig und Berlin; 1907.
135. Faxén, H. PhD thesis. Uppsala: 1921.
136. Faxén H. Arkiv Mat Astrom Fys. 1923; 17:1.
137. Oseen, CW. Neuere Method und Ergebnisse in der Hydrodynamik. Akademische Verlagsgeselleschat M B H; Leipzig: 1927.
138. Wakiya S. Res Rep Fac Eng., Niigata Univ. 1960; 9:31.
139. Happel, J., Brenner, H. Low Reynolds number hydrodynamics: with special applications to particulate media. Martinus Nijhoff Publishers; The Hague: 1983. First paperback edn
140. Perkins GS, Jones RB. Physica A. 1992; 189:447–477.
141. Carbajal-Tinoco MD, Lopez-Fernandez R, Arauz-Lara JL. Phys Rev Lett. 2007; 99:138303. [PubMed: 17930646]
142. Brenner H. Chem Eng Sci. 1961; 16:242–251.
143. Maude AD. Br J Appl Phys. 1961; 12:293.
144. MacKay GDM, Suzuki M, Mason SG. J Colloid Sci. 1963; 18:103–104.

145. Honig EP, Roebersen GJ, Wiersema PH. J Colloid Interface Sci. 1971; 36:97–109.
146. Bevan MA, Prieve DC. J Chem Phys. 2000; 113:1228–1236.
147. Richardson S. J Fluid Mech. 1973; 59:707–719.
148. De Gennes PG. Langmuir. 2002; 18:3413–3414.
149. Choi CH, Westin KJA, Breuer KS. Phys Fluids. 2003; 15:2897–2902.
150. Lauga, E., Brenner, MP., Stone, HA. Handbook of experimental fluid mechanics. Springer; 2005. p. 1219-1240.ch. 19
151. Neto C, Evans DR, Bonaccurso E, Butt HJ, Craig VSJ. Rep Prog Phys. 2005; 68:2859.
152. Bocquet L, Barrat JL. Soft Matter. 2007; 3:685–693.
153. Zhu Y, Granick S. Phys Rev Lett. 2001; 87:096105. [PubMed: 11531582]
154. Lauga E, Brenner MP. Phys Rev E: Stat, Nonlinear, Soft Matter Phys. 2004; 70:026311.
155. Lauga E, Squires TM. Phys Fluids. 2005; 17:103102.
156. Lin B, Yu J, Rice SA. Phys Rev E: Stat Phys, Plasmas, Fluids, Relat Interdiscip Top. 2000; 62:3909–3919.
157. Jeney S, Lukić B, Kraus JA, Franosch T, Forró L. Phys Rev Lett. 2008; 100:240604. [PubMed: 18643565]
158. Bian X, Litvinov S, Qian R, Ellero M, Adams NA. Phys Fluids. 2012; 24:012002.
159. Saugey A, Joly L, Ybert C, Barrat JL, Bocquet L. J Phys: Condens Matter. 2005; 17:S4075.
160. Wakiya S. Res Rep Fac Eng, Niigata Univ. 1961; 10:15.
161. Wakiya S. J Phys Soc Jpn. 1964; 19:1401–1408.
162. Gotoh TI, Kaneda Y. J Chem Phys. 1982; 76:3193–3197.
163. Pagonabarraga I, Hagen MHJ, Lowe CP, Frenkel D. Phys Rev E: Stat Phys, Plasmas, Fluids, Relat Interdiscip Top. 1998; 58:7288–7295.
164. Felderhof BU. J Phys Chem B. 2005; 109:21406–21412. [PubMed: 16853777]
165. Huang K, Szlufarska I. Nat Commun. 2015; 6:8588. [PubMed: 26446866]
166. Franosch T, Jeney S. Phys Rev E: Stat, Nonlinear, Soft Matter Phys. 2009; 79:031402.
167. Crocker JC. J Chem Phys. 1997; 106:2837–2840.
168. Dufresne ER, Squires TM, Brenner MP, Grier DG. Phys Rev Lett. 2000; 85:3317–3320. [PubMed: 11019330]
169. Dufresne ER, Altman D, Grier DG. Europhys Lett. 2001; 53:264.
170. Kim, S., Karrila, SJ. Microhydrodynamics: principles and selected applications. Dover Publications, Inc.; Mineola, New York: 2005.
171. Kao MH, Yodh AG, Pine DJ. Phys Rev Lett. 1993; 70:242–245. [PubMed: 10053738]
172. Hagen MHJ, Pagonabarraga I, Lowe CP, Frenkel D. Phys Rev Lett. 1997; 78:3785–3788.
173. Henderson S, Mitchell S, Bartlett P. Phys Rev Lett. 2002; 88:088302. [PubMed: 11863977]
174. Bakker AF, Lowe CP. J Chem Phys. 2002; 116:5867–5876.
175. Felderhof BU. J Chem Phys. 2005; 123:184903. [PubMed: 16292935]
176. Felderhof BU. J Chem Phys. 2012; 136:012002.
177. Zwanzig R. Physica A. 1983; 118:427–433.
178. Thompson PA, Troian SM. Nature. 1997; 389:360–362.
179. Granick S, Zhu Y, Lee H. Nat Mater. 2003; 2:221–227. [PubMed: 12690393]
180. Asproulis N, Drikakis D. Phys Rev E: Stat, Nonlinear, Soft Matter Phys. 2011; 84:031504.
181. Felderhof BU. Phys Rev E: Stat., Nonlinear, Soft Matter Phys. 2012; 85:046303.
182. Thompson PA, Robbins MO. Phys Rev A: At, Mol, Opt Phys. 1990; 41:6830–6837.
183. Kim C, Karniadakis GE. J Stat Phys. 2015; 158:1100–1125.
184. Ermak DL, McCammon JA. J Chem Phys. 1978; 69:1352–1360.
185. Brady JF, Bossis G. Annu Rev Fluid Mech. 1988; 20:111–157.
186. Swan JW, Brady JF. Phys Fluids. 2007; 19:113306.
187. Maxey MR, Patel BK. Int J Multiphase Flow. 2001; 27:1603–1626.
188. Liu D, Keaveny E, Maxey MR, Karniadakis GE. J Comput Phys. 2009; 228:3559–3581.

189. Keaveny EE. J Comput Phys. 2014; 269:61–79.
190. Allen, MP., Tildesley, DJ. Computer simulation of liquids. Clarendon Press; Oxford: 1989.
191. Frenkel, D., Smit, B. Understanding molecular simulation: from algorithms to applications. Academic Press, a division of Harcourt, Inc; 2002.
192. Atzberger PJ, Kramer PR, Peskin CS. J Comput Phys. 2007; 224:1255–1292.
193. Sharma N, Patankar NA. J Comput Phys. 2004; 201:466–486.
194. Usabiaga FB, Pagonabarraga I, Delgado-Buscalioni R. J Comput Phys. 2013; 235:701–722.
195. Usabiaga FB, Delgado-Buscalioni R, Griffith BE, Donev A. Comput Methods Appl Mech Eng. 2014; 269:139–172.
196. Ladd AJC. Phys Rev Lett. 1993; 70:1139–1342. [PubMed: 10054296]
197. Ladd AJC. J Fluid Mech. 1994; 271:285–309.
198. Pan W, Caswell B, Karniadakis GE. Langmuir. 2009; 26:133–142.
199. Vázquez-Quesada A, Ellero M, Español P. Microfluid Nanofluid. 2012; 13:249–260.
200. Malevanets A, Kapral R. J Chem Phys. 2000; 112:7260–7269.
201. Padding JT, Louis AA. Phys Rev E: Stat, Nonlinear, Soft Matter Phys. 2006; 74:031402.
202. Gompper, G., Ihle, T., Kroll, D., Winkler, R. Advanced computer simulation approaches for soft matter sciences III. Vol. 221. Springer; Berlin Heidelberg: 2009. p. 1-87.

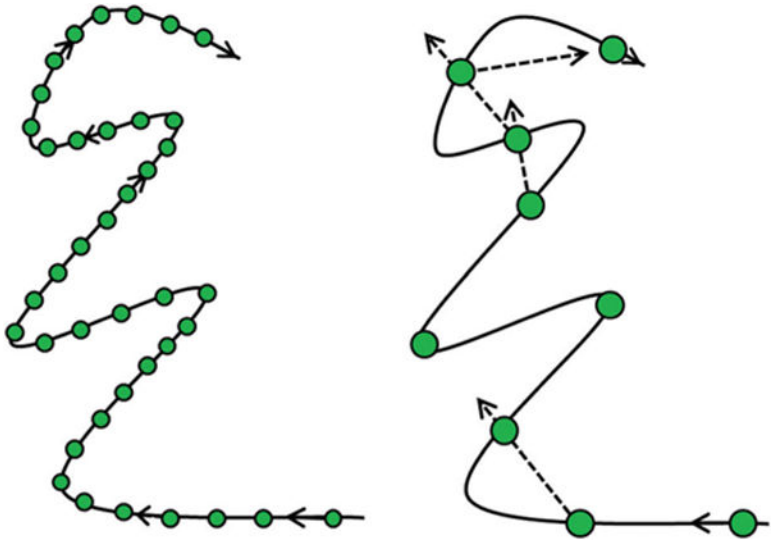

Fig. 1.

Fractal trajectory of Brownian motion according to Einstein's diffusion model in two dimensions. On the left is the actual trajectory of a particle. On the right are the observed locations of the particle on diffusive time scales. Arrows indicate the apparent velocities of the particle.

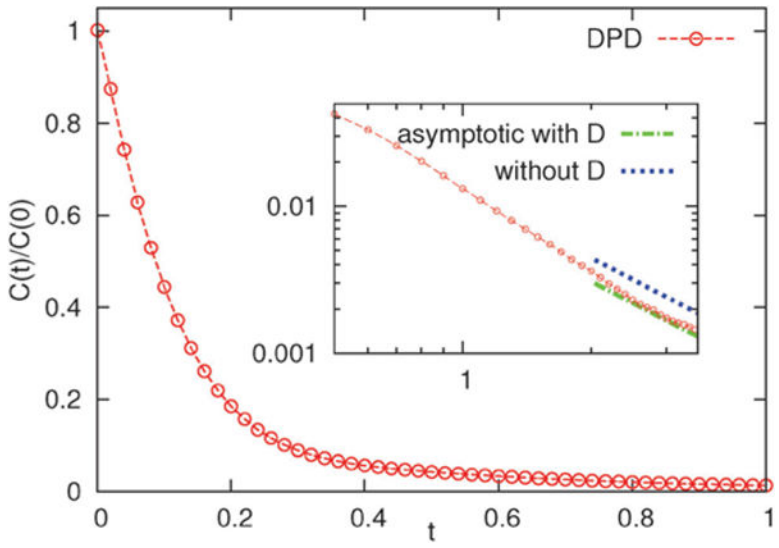

Fig. 2.

Asymptotic limit of the velocity autocorrelation function for a diffusive particle. Eqn (33) with or without diffusion coefficient D is compared with the results of tagged fluid particles in dissipative particle dynamics (DPD) simulations. The inset shows the long-time limit in the logarithmic scale. Input parameters of DPD are taken from a previous work,[105,106] which correspond to a fluid with $k_B T = 1$, $\rho = 3$, $v = 0.54$, and $D = 0.15$ in DPD units.

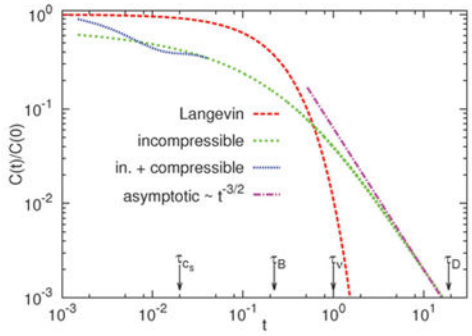

(a) $C(t)$: Langevin — Eq. (25); incompressible — Eq. (34); in. + compressible — sum of incompressible contribution Eq. (34) and compressible contribution Eq. (36); asymptotic — Eq. (33) with $D = 0$.

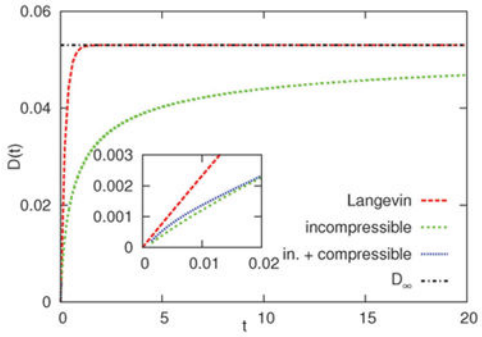

(b) $D(t)$: Langevin — Eq. (27); incompressible — time integral of Eq. (34); in. + compressible — time integral of Eq. (34) + Eq. (36); D_∞ — Eq. (7). The inset indicates differences of diffusion coefficients at short time.

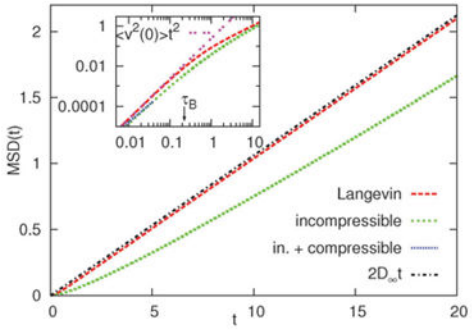

(c) $\langle \Delta x^2(t) \rangle$: Langevin — Eq. (17); incompressible — Eq. (35) with Eq. (34); in. + compressible — Eq. (35) with Eqs. (34) and (36).The inset indicates differences of MSDs at short time.

Fig. 3.

C(t), D(t), and $\langle \Delta x^2(t) \rangle$ of a Brownian particle (1D) according to the Langevin model, incompressible viscous hydrodynamics, and its correction due to compressible effects at the short time scale. Relevant time scales are sonic time $\tau_{c_s} = a/c_s$, viscous time $\tau_\nu = a^2/\nu$, Brownian relaxation time $\tau_B = m/\xi$, and diffusive time $\tau_D = a^2/D_\infty$. The definitions of variables are in the text. For a demonstrative purpose their values are $a = 1$, $c_s = 50$, $\rho = \rho_B = 1$, $\nu = 1$, and $k_B T = 1$ in reduced units. Hence $\tau_{c_s} = 0.02$, $\tau_B = 0.22$, $\tau_\nu = 1.0$, and $\tau_D = 18.85$.

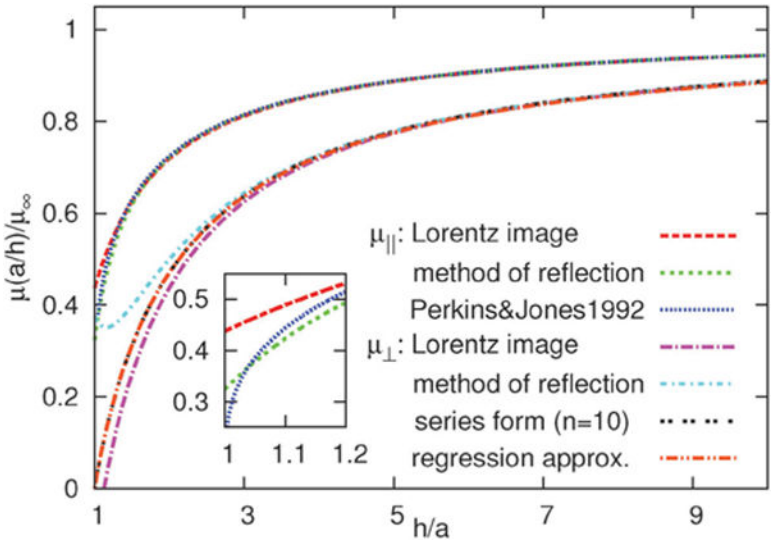

Fig. 4.

Mobility of a sphere near a no-slip wall. The results from Lorentz's image technique are taken up to the first order of a/h in eqn (37) and (38); the results from the method of reflection are the complete expressions in eqn (37) and (38). The prediction of $\mu_{\parallel}$ in eqn (39) from Perkins and Jones is shown to be more accurate at the short distance, as indicated in the inset. The prediction of $\mu_{\perp}$ with series solution is taken from eqn (40) up to $n = 10$ and including higher n does not change the sum of series significantly. The regression approximation for $\mu_{\perp}$ in eqn (41) is almost identical to the series solution.

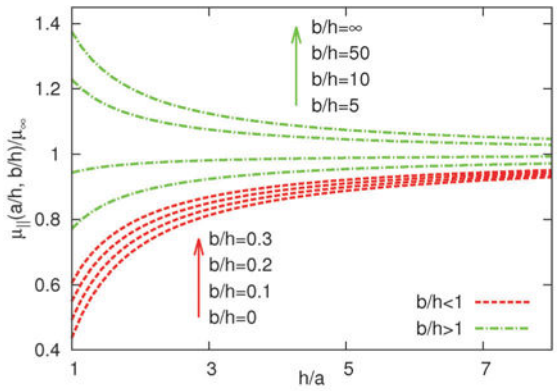

(a) Parallel: $b < h$ from Eq. (43); $b > h$ from Eq. (45).

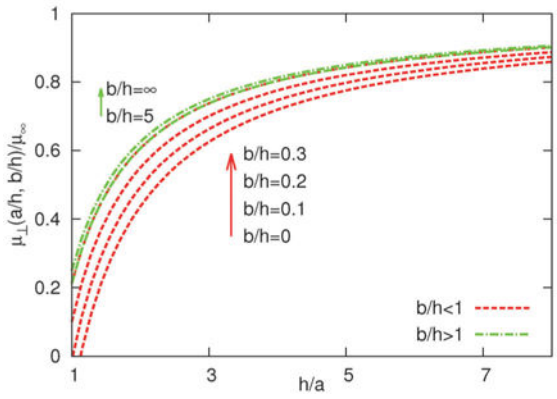

Fig. 5.
Mobility of a sphere near a slip wall.